SUPPLEMENTAL FIGURES

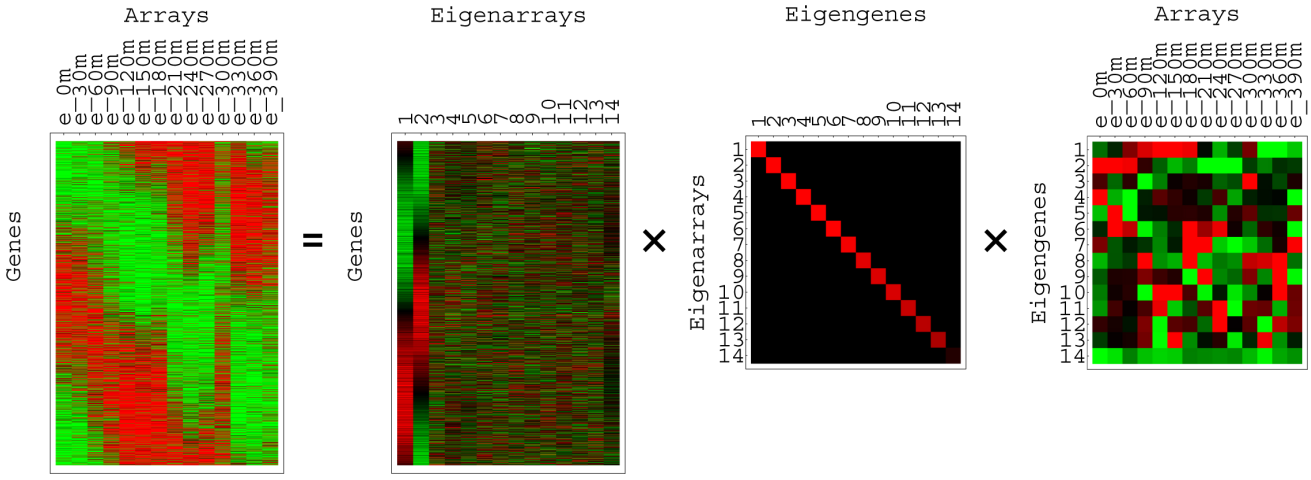

FIG. 13: SVD of the normalized and sorted elutriation data. Raster display of $\hat{e}_N = \hat{u}_N\,\hat{\varepsilon}_N\,\hat{v}_N^T$ with overexpression (red), no change in expression (black), and underexpression (green) around the steady state of expression, showing linear transformation of the data from the 6018-genes × 14-arrays space to the reduced diagonalized 14-eigenarrays × 14-eigengenes space using the 6018-genes × 14-eigenarrays and 14-eigengenes × 14-arrays basis sets.

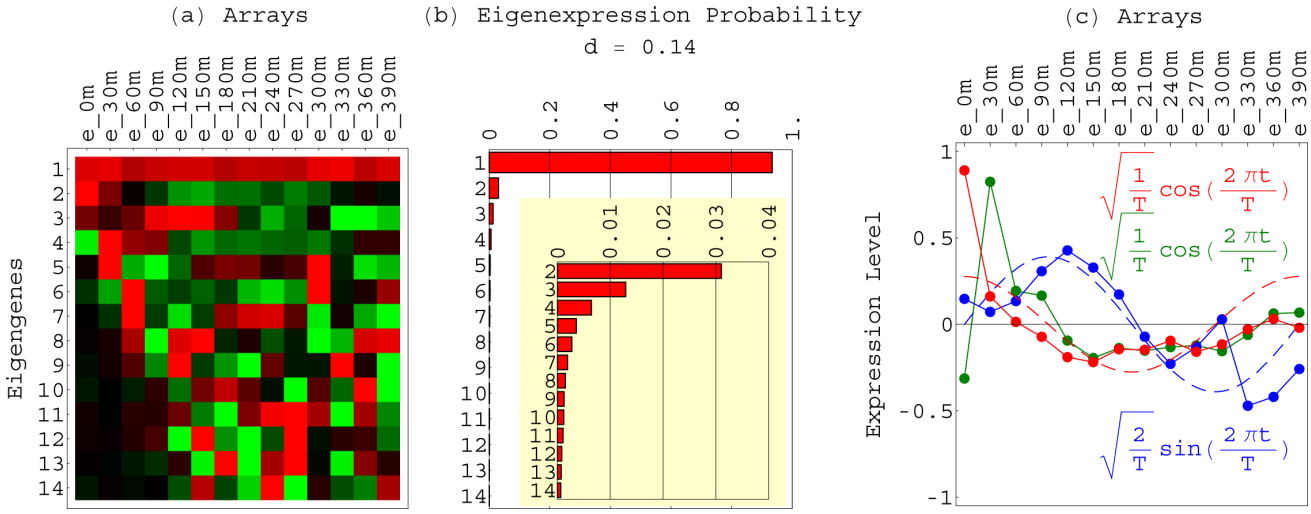

FIG. 14: Elutriation eigengenes. (*a*) Raster display of $\hat{v}^T$, the expression of 14 eigengenes in 14 arrays, with overexpression (red), no change in expression (black), and underexpression (green) around the steady-state expression, which can be associated with the first eigengene, $|\gamma_1\rangle$. (*b*) Bar chart of the probability of eigenexpression p_l of each eigengene $|\gamma_l\rangle$, showing more than 90% of the overall relative expression in $|\gamma_1\rangle$, about 3%, 1.5%, and 0.5% in $|\gamma_2\rangle$, $|\gamma_3\rangle$, and $|\gamma_4\rangle$, respectively, and a low entropy $d = 0.14 \ll 1$. (*c*) Line-joined graphs of the expression levels of $|\gamma_2\rangle$ (red), $|\gamma_3\rangle$ (blue), and $|\gamma_4\rangle$ (green) in the 14 arrays, and dashed graphs of normalized cosine (blue) and sine (red) of period T.

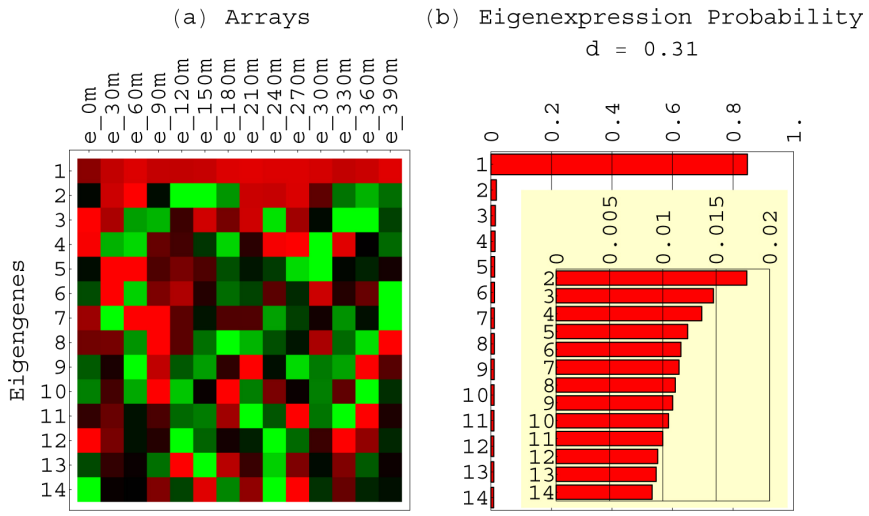

FIG. 15: Eigengenes of the natural logarithm of the variances in elutriation expression $\hat{e}_{LV}$. (*a*) Raster display of $\hat{v}^T_{LV}$; $|\gamma_1\rangle_{LV}$ is inferred to represent the steady scale of expression variance. (*b*) $|\gamma_1\rangle_{LV}$ captures more than 80% of the overall information in this dataset.

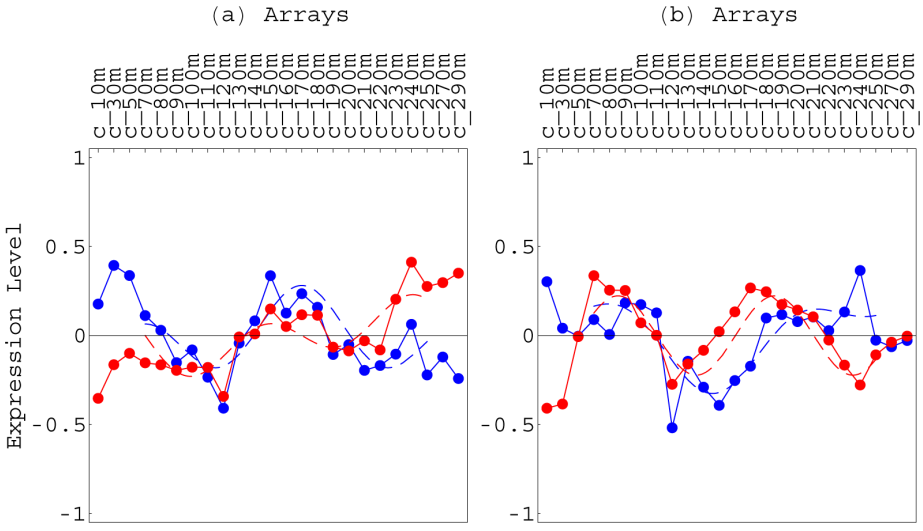

FIG. 16: *CDC15* eigengenes. (*a*) Line-joined graphs of the expression levels of $|\gamma_3\rangle$ (red) and $|\gamma_4\rangle$ (blue). (*b*) Expression levels of $|\gamma_5\rangle$ (red) and $|\gamma_6\rangle$ (blue). All fit dashed graphs of periodic functions with period $2T/5 \approx 120$m superimposed on periodic functions with period $4T/5 \approx 240$m during the cell cycle.

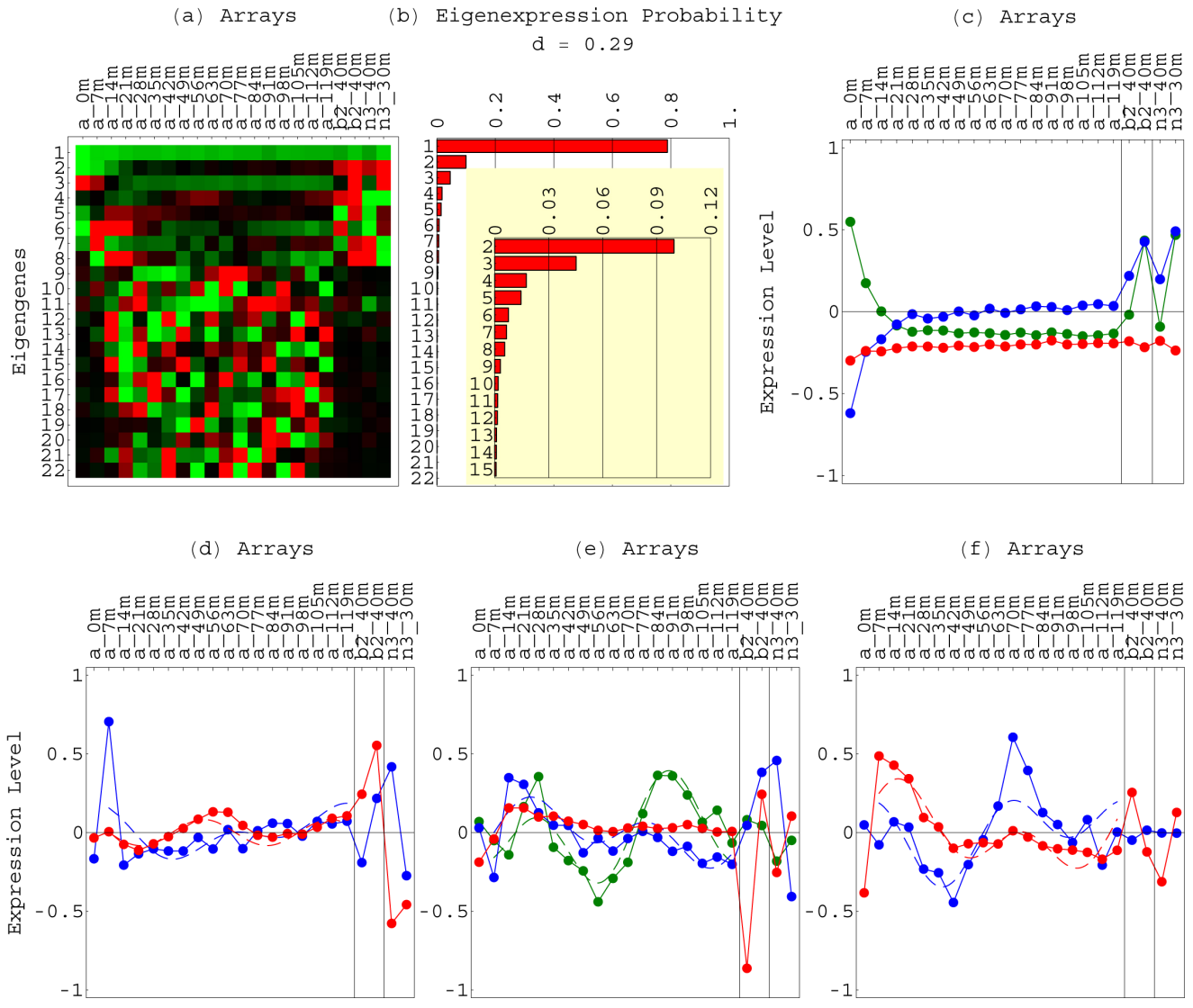

FIG. 17: α factor, *CLB2*, and *CLN3* eigengenes. (*a*) Raster display of $\hat{v}^T$, the expression of 22 eigengenes in 22 arrays. (*b*) Bar chart of the probabilities of eigenexpression, showing that $|\gamma_1\rangle$ captures about 80% of the overall relative expression. (*c*) Line-joined graphs of the expression levels of $|\gamma_1\rangle$ (red), which is inferred to represent the steady expression state, and $|\gamma_2\rangle$ (blue) and $|\gamma_3\rangle$ (green), which are inferred to represent responses to synchronization in the cell cycle. (*d*) Expression levels of $|\gamma_4\rangle$ (red) and $|\gamma_7\rangle$ (blue). (*e*) Expression levels of $|\gamma_5\rangle$ (red), $|\gamma_8\rangle$ (blue), and $|\gamma_{11}\rangle$ (green). (*f*) Expression levels of $|\gamma_6\rangle$ (red) and $|\gamma_9\rangle$ (blue). All fit dashed graphs of periodic functions with period $T/2 = 66$m superimposed on periodic functions with period $T = 112$m from $t = 7$ to $t = 119$m during the cell cycle.

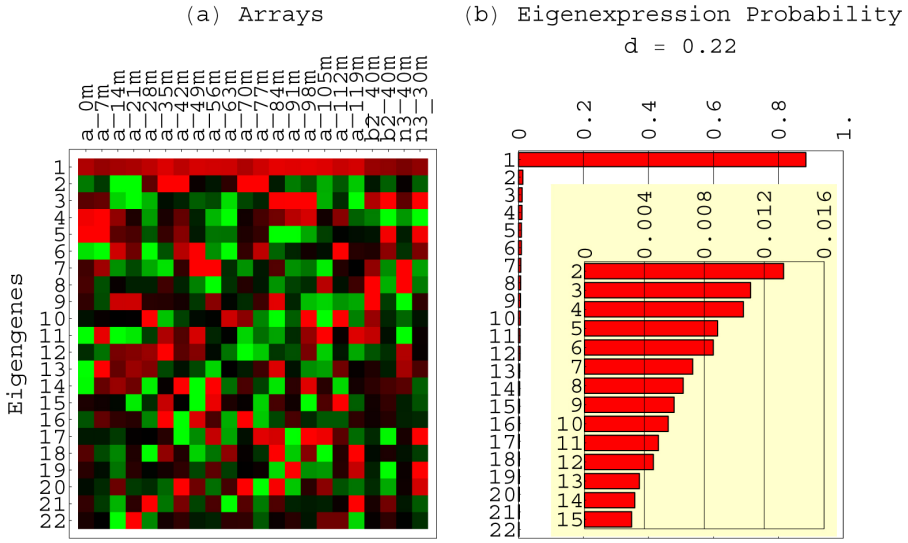

FIG. 18: Eigengenes of the natural logarithm of the variances in expression in the α factor, *CLB2*, and *CLN3* experiments $\hat{e}_{LV}$. (*a*) Raster display of $\hat{v}_{LV}^T$; $|\gamma_1\rangle_{LV}$ is inferred to represent the steady scale of expression variance. (*b*) $|\gamma_1\rangle_{LV}$ captures about 90% of the overall information in this dataset.